IEEE Photonics Journal
An IEEE Photonics Society Publication

Open Access

Phase-Shift Method-Based Optical VSB Modulation Using High-Pass Hilbert Transform

Volume 8, Number 5, October 2016

K. I. Amila Sampath, *Student Member, IEEE*
Katsumi Takano, *Senior Member, IEEE*

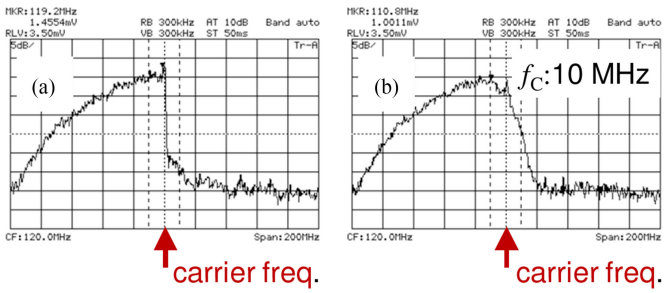

DOI: 10.1109/JPHOT.2016.2603236
1943-0655 © 2016 IEEE

IEEE photonics SOCIETY

IEEE

Phase-Shift Method-Based Optical VSB Modulation Using High-Pass Hilbert Transform

K. I. Amila Sampath *Student Member, IEEE*, and Katsumi Takano, *Senior Member, IEEE*

Department of Electrical Engineering, Yamagata University, Yonezawa, Yamagata, Japan.

DOI:10.1109/JPHOT.2016.2603236

Manuscript received July 8, 2016; revised August 22, 2016; accepted August 22, 2016. Date of publication August 26, 2016; date of current version September 19, 2016. This work was supported in part by Ministry of Education, Culture, Sports, Science, and Technology in Japan (KAKENHI No. 15K13985) and in part by the Sato Yo International Scholarship Foundation (No. 644). Corresponding author: K. I. Amila Sampath (e-mail: KIAmila.Sampath.jp@ieee.org).

Abstract: This report presents a novel method of generating an optical vestigial sideband (VSB) modulated signal without using optical bandpass filters. Using a modified Hilbert transformer based on digital signal processing, an optical VSB-modulated signal is generated using the phase-shift method. The proposed method is demonstrated experimentally for an optical binary phase-shift keying (BPSK) signal. The proposed method is wavelength-transparent compared to an optical bandpass filtering method, where the wavelength dependence of the optical bandpass filter limits applications. Furthermore, the optical bandwidth of the modulated signal is readily adjustable by changing the cutoff frequency of the high-pass Hilbert transformer. Fiber transmission characteristics of a single-channel optical BPSK-VSB signal are analyzed using a 100-km transmission link. Results of fiber transmission analysis show tolerance of the proposed modulation scheme to fiber nonlinearity-based signal distortions. For a 10 Gbit/s non-return-to zero(NRZ) sequence, a self-phase modulation threshold of 13 dBm is reported for the studied system.

Index Terms: Optical communications, binary phase-shift keying optical vestigial sideband (BPSK-VSB), BPSK single-sideband (SSB), fiber transmission, homodyne detection, peak-to-average power ratio (PAPR).

1. Introduction

Increased spectral efficiency is regarded as a key approach to implementing high-capacity optical transmission systems [1], [2]. Sophisticated digital signal processing (DSP) contributes greatly to increased spectral efficiency in state-of-the art long- haul optical communication systems [3]–[6]. Intensity modulation-direct detection (IM-DD) technologies such as pulse amplitude modulation (PAM), carrier-less amplitude/phase modulation (CAP) and discrete multitone (DMT) modulation are being studied for short-reach applications where the cost becomes a major factor [7], [8]. PAM is very attractive for short-reach applications ($<$10 km) because of its cost performance. Nevertheless, low receiver sensitivity limits the reach of PAM [9]. DMT modulation is being studied to increase the reach [10]. Higher spectral efficiency and tolerance to differential group delay (DGD) of DMT makes it an ideal candidate for longer transmission distance. However, frequency related power fading of DMT subcarriers becomes a serious issue especially after 80-km transmission [11].

Because of their characteristic high spectral efficiency, optical single-sideband (SSB) and vestigial sideband (VSB) modulations were studied when DSP was less advanced [12]–[18]. Actually, SSB modulation cannot exceed the spectral efficiency of double-sideband (DSB) modulation of complex baseband signal (IQ modulation) [19]. However, dispersion compensation of carrier-emitted optical SSB/VSB modulated signal can be done in the electrical domain after direct detection using simple techniques such as microstrip lines [12], [13]. In addition, optical SSB/VSB modulation shows tolerance against DGD and polarization mode dispersion (PMD) [18], [20]. Those benefits make carrier-emitted optical SSB/VSB modulation cost effective for short-reach applications. On the other hand, carrier-suppressed optical SSB/VSB modulation with coherent detection can increase both power and spectral efficiencies in medium/long-reach transmission. In carrier suppressed optical SSB/VSB modulation, the entire energy being transmitted is used for data transmission [21]. Compared with optical IQ modulation with sophisticated DSP, carrier-suppressed optical SSB/VSB modulation presents the advantages of higher receiver sensitivity, simple receiver structure and less burden on DSP. These characteristics of carrier-suppressed optical SSB/VSB modulation make it a promising candidate for low cost medium-reach networks. Nevertheless, the difficulty of implementing optical bandpass filters with sharp roll-off characteristics [22] and performance degradation caused by filtering in the optical domain [16], [18] have prevented the wider use of optical SSB modulation for commercial optical communication systems. Optical VSB modulation using an optical bandpass filter depends mainly on the optical bandpass filter characteristics [17], [18]. Phase fluctuations occurring because of optical filtering near the carrier frequency severely degrade the optical VSB signal. When severe signal distortion occurs because of optical filtering, electrical equalizers with wider bandwidth must be used to equalize the filtered signal [17]. Also in such cases, the frequency stability of the light source and the filter's ability of frequency locking to the light source are crucially important [16], [18]. Experiment results for optical VSB modulation reported in the literature suggest performance enhancement capability by improving optical bandpass filter properties [14]–[16], [20], [23].

Instead of filtering out a particular frequency band of the modulated signal using an optical bandpass filter, spectral suppression can be achieved using phase-shift method [24]. In phase-shift method, spectral suppression is implemented using Hilbert transform. Hilbert transform, which can be implemented easily using DSP [25], creates π phase difference around the center frequency of the baseband signal spectrum. Therefore, adding a Hilbert transformed signal to its original achieves spectral suppression. Using phase-shift method, spectral suppression can be implemented with no phase fluctuation [26]. For the first time, we demonstrated phase-shift method optical BPSK-VSB modulation using modified Hilbert transform in an earlier report [27]. When using optical filtering, the freedom of wavelength tunability is limited primarily by the wavelength dependence of the optical band-pass filter. Our method is wavelength-transparent because spectral suppression is implemented using DSP, irrespective of the optical carrier wavelength. Capability of transmitter imperfection compensation using DSP also might be an advantage of phase-shift method optical VSB modulation. Signal distortions by phase fluctuations caused by optical filtering can also be avoided using the proposed method. Adaptivity of the channel bandwidth and the optical signal-to-noise ratio (OSNR) can be regarded as particular benefits of phase-shift method optical VSB modulation. Compared with optical filtering method, high order harmonics due to modulator nonlinearity might be a trade-off in phase-shift method optical VSB modulation.

This paper is an extension of an earlier report [27] that included details of the principle of optical VSB modulation using phase-shift method. In this paper, we propose phase-shift method based optical BPSK-VSB modulation as a cost effective option to increase the reach over 80-km. Instead of IM-DD technologies, we use optical BPSK modulation to increase the receiver sensitivity. Taking the advantage of digital coherent detection, we examined unamplified transmission for medium-reach networks. Cross phase modulation (XPM) based signal distortion is expected to be a dominant factor in wavelength division multiplexed (WDM) SSB/VSB transmission. However, to clarify the self-phase modulation (SPM)-induced signal impairments of the proposed modulation scheme, we conducted single-channel fiber transmission analysis as the first stage.

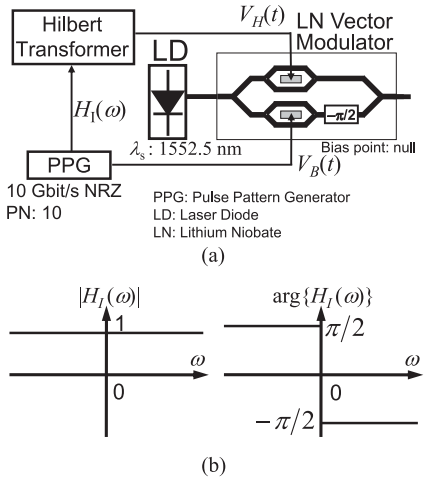

Fig. 1. (a) Phase-shift method optical single-sideband transmitter model. (b) Hilbert transforms transfer function.

The remainder of this paper is organized as follows. Section 2 presents the principle of phase-shift method optical VSB modulation. A proof-of-principle experiment and its results are described in Section 3. The numerically analyzed transmission performance of the phase-shift method optical VSB signal is explained in Section 4 before conclusions are presented.

2. Optical VSB Modulation Based on Phase-shift Method

After explaining some characteristics of the modulator output signal when an ideal Hilbert transformer is used, the principle of phase-shift method optical VSB modulation is explained. When an ideal Hilbert transformer is used, the modulator output becomes the optical SSB modulated signal.

2.1 Phase-Shift Method Optical SSB Modulation

Using the phase-shift method, spectral suppression can be implemented by adding an orthogonally modulated baseband signal to its Hilbert transform. The Hilbert transform defined in (1), shown below, creates π phase-shift around the center frequency of the baseband spectrum.

$$H_I(\omega) = \begin{cases} -j\,\mathrm{sgn}(\omega), & (\omega \neq 0) \\ 0, & (\omega = 0) \end{cases} \tag{1}$$

In (1), sgn(·) is the signum function, and ω is the angular frequency. Because of the phase shift created by the Hilbert transform, adding the baseband signal to the Hilbert-transformed signal produces a sideband-suppressed signal. The sideband-suppressed signal produced using phase-shift method can be generated using the transmitter model presented in Fig. 1(a) [28]. Two subMach-Zehnder interferometers (MZIs) of the Lithium niobate (LN) vector modulator are driven by baseband signal $V_B(t)$ and its Hilbert transform $V_H(t)$. Along with spectral suppression, carrier suppression can also be achieved by biasing both subMZIs to their transmission null points. If the Hilbert transformer gives the ideal response presented in Fig. 1(b), then the modulator output signal bandwidth becomes one-half of the double-sideband modulation. Therefore, it is designated as a single-sideband signal. The modulator output signal power spectrum, its waveform, and modulator driving signal waveforms are presented in Fig. 2 when the ideal Hilbert transform is used. The power spectrum of the intensity-modulated signal is also presented in Fig. 2(a) for comparison. Spectral suppression greater than 48 dB is achieved using phase-shift method. The baseband signal is a binary sequence. The optical carrier is suppressed during modulation. Therefore, this modulation can be designated as optical BPSK-SSB modulation. Among the driving signals, peaks are apparent

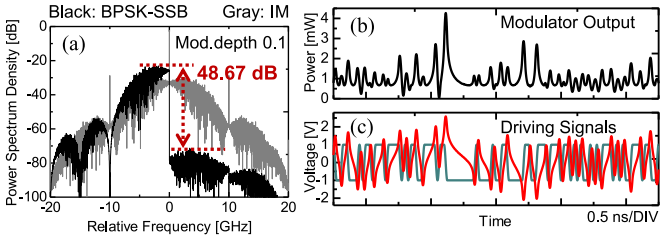

Fig. 2. (a) Power spectra of optical BPSK-SSB signal and intensity modulated signal. (b) Optical waveform of modulator output. (c) Modulator driving signals (green, baseband signal; red, Hilbert-transformed signal).

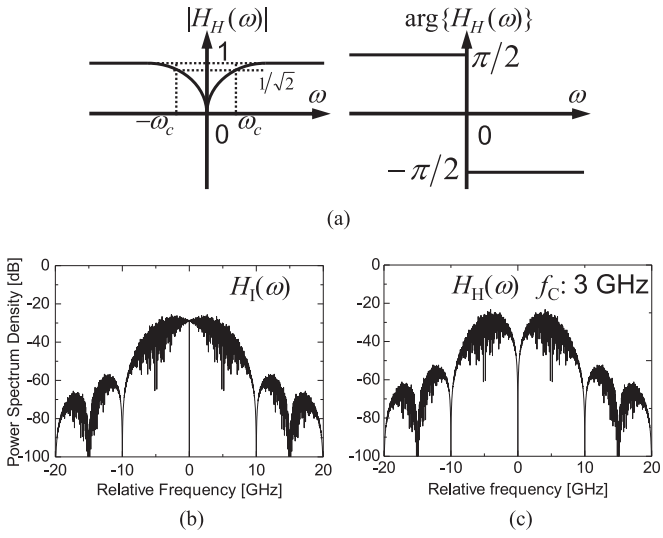

Fig. 3. (a) High-pass Hilbert transformers transfer function. (b) Power spectra of $H_I(\omega)$. (c) Power spectra of $H_H(\omega)$ (f_C: 3 GHz).

in the Hilbert-transformed waveform at the transition points of the baseband signal between marks and spaces [29]. The modulator output optical waveform becomes peaky because of the peaks of the Hilbert-transformed waveform. Peak-to-average power ratio (PAPR) of the modulator output signal becomes high because of these peaks from the Hilbert-transformed waveform. Because of high PAPR, SPM-induced nonlinear phase-shifts degrade the optical BPSK-SSB signal during fiber transmission [29], [30].

We define the modulation depth as the ratio of the baseband signal peak voltage (V_{B-Peak}) to V_π, where V_π is the half-wave voltage of the LN modulator. When an ideal Hilbert transformer is used, the peak-to-peak voltage of the Hilbert-transformed signal component (V_{pp-H}) becomes 2.5 times that of the baseband signal (V_{pp-B}). Modulator nonlinearity limits the maximum peak-to-peak driving signal voltage to $2V_\pi$. Therefore, the modulation depth is restricted to 0.4 in an ideal Hilbert transformer case [28].

2.2 Phase-Shift Method Optical VSB Modulation

Associated shortcomings of the phase-shift method optical BPSK-SSB modulation described above can be overcome by shifting the SSB modulation to VSB modulation at the expense of spectral broadening. An optical VSB modulated signal using phase-shift method can be generated by manipulating the amplitude response of the Hilbert transformer. The manipulated response of Hilbert transformer is depicted in Fig. 3(a). The amplitude response of the ideal Hilbert transformer

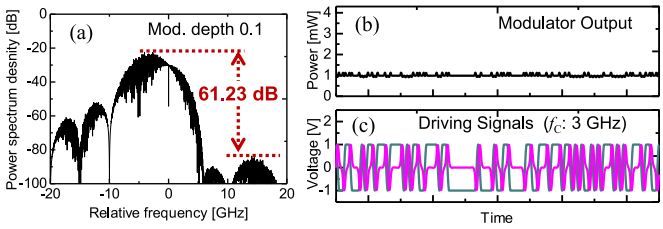

Fig. 4. (a) Power spectra of optical BPSK-VSB signal. (b) Optical waveform of modulator output. (c) Modulator driving signals (green, baseband signal; pink, high-pass Hilbert-transformed signal).

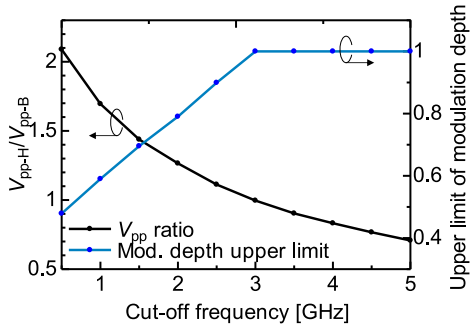

Fig. 5. Relation of high-pass Hilbert transform cut-off frequency with driving signal voltage ratio and the upper limit of the modulation depth (10 Gbit/s NRZ coded baseband signal).

is changed to high-pass response while the phase response remains unchanged. Modified Hilbert transform is defined as $H_H(\omega)$ in (2). Here, ω_c is the angular cut-off frequency.

$$H_H(\omega) = \begin{cases} -j\,\mathrm{sgn}(\omega), & (|\omega| > 2\omega_c) \\ -j\,\mathrm{sgn}(\omega)\sin\left\{\pi\left\{\frac{|\omega|}{4\omega_c}\right\}\right\}, & (|\omega| \le 2\omega_c) \end{cases} \tag{2}$$

Because of the high-pass amplitude response, we call the modified Hilbert transform a high-pass Hilbert transform. Power spectrum of a high-pass Hilbert transformed signal is presented with that of the ideal Hilbert transform in Fig. 3 for comparison. The input of the Hilbert transformer is a 10 Gbit/s non-return-to zero (NRZ) sequence. The cut-off frequency (f_C) of the high-pass Hilbert transformer is 3 GHz. The high-pass amplitude response reduces the power of the low-frequency components of the Hilbert-transformed signal, in which the energy is concentrated. This power reduction of low-frequency components suppresses the peaks in the Hilbert-transformed waveform. When high-pass Hilbert transforms are used, the driving signals and modulator output optical waveform of 10 Gbit/s NRZ sequence are as depicted in Fig. 4, where f_C of $H_H(\omega)$ is 3 GHz. Compared with the optical BPSK-SSB spectrum in Fig. 2(a), higher spectral suppression can be observed in the modulator output signal spectrum with fewer high-order harmonics. However, the main lobe bandwidth of Fig. 4(a) widens. The spectral imbalance caused by high-pass filtering between the baseband signal and high-pass Hilbert transformed signal produces an optical spectrum with a vestigial sideband. Therefore, this optical signal is designated as a phase-shift method optical BPSK-VSB signal. V_{pp-H} becomes equal to V_{pp-B} for f_C of 3 GHz. Consequently, the peaks of the modulator output waveform disappear in the high-pass Hilbert transform waveform.

2.3 Characteristics of the Phase-Shift Method Optical BPSK-VSB Signal

Characteristic dependence of the phase-shift method optical BPSK-VSB signal on the cut-off frequency of the high-pass Hilbert transform and modulation depth were examined. The driving signal voltage ratio and the upper limit of the modulation depth of the phase-shift method optical BPSK-VSB signal are presented in Fig. 5. With increasing cut-off frequency, the peaks of the

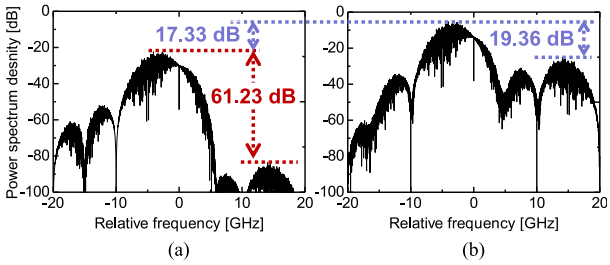

Fig. 6. Power spectra comparison of optical BPSK-VSB signal at different modulation depths (f_C: 3 GHz). (a) Modulation depth 0.1. (b) Modulation depth 1.0.

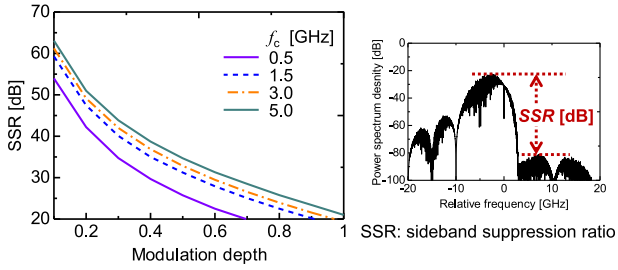

Fig. 7. Sideband suppression ratio (SSR) of optical BPSK-VSB signal. (Inset) Definition of SSR.

Hilbert-transformed signal are reduced. The driving signal voltage ratio is reduced accordingly. For the 10 Gbit/s NRZ sequence, the driving signal voltage ratio reaches 1 at the cut-off frequency of 3 GHz, where V_{pp-H} equals V_{pp-B}. An additional increase of the cut-off frequency makes V_{pp-H} smaller than V_{pp-B}. Reduction of V_{pp-H}, the limiting factor of modulation depth, allows an increase of the modulation depth. The maximum modulation depth of 1.0 can be achieved at cut-off frequencies of 3 GHz. Actually, V_{pp-H} becomes smaller than V_{pp-B} for cut-off frequencies higher than 3 GHz. Therefore, the modulation depth can be set to its maximum level.

Effects of modulation depth on the phase-shift method optical BPSK-VSB signal are presented for comparison in Fig. 6. Fig. 6(a) depicts the power spectrum of optical BPSK-VSB signal (f_C: 3 GHz) at modulation depth of 0.1, where the spectral suppression becomes 61.23 dB. The power spectrum of the modulator output signal at modulation depth of 1.0 is shown in Fig. 6(b). A power increase of 17.33 dB in the main lobe of the spectrum can be observed to occur with increased modulation depth. While increasing the main lobe power, increased modulation depth results decreased the spectral suppression. Because of the modulator nonlinearity, the increased modulation depth brings spurious spectral components to the spectrum, which reduces the spectral suppression. However, spectral suppression over 19 dB is observed even at the modulation depth of 1.0. The sideband suppression ratio (SSR) is defined as the difference between the maximum power spectral densities of the main lobe and the side lobe with the highest power (see the inset of Fig. 7). Fig. 7 shows the SSR of the optical BPSK-VSB signal against the modulation depth for various cut-off frequencies of the high-pass Hilbert transformer. Because of the power increase at high frequencies attributable to the nonlinearity of the modulator, SSR degrades with increasing modulation depth. However, increasing cut-off frequency reduces V_{pp-H}, which reduces SSR degradation by high-order harmonics.

3. Proof of Principle Experiment

3.1 Experiment

This experiment was conducted to demonstrate the phase-shift method of optical VSB modulation experimentally. The optical BPSK-VSB signal characteristics were elucidated. The experimental setup is presented in Fig. 8. Driving signals were generated by two synchronized arbitrary

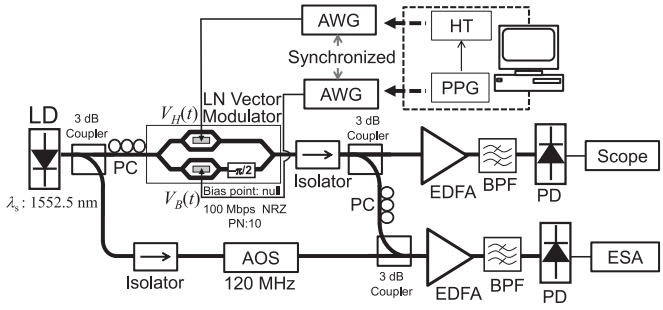

Fig. 8. Experimental setup: AOS, acousto-optic switch; AWG, arbitrary waveform generator; BPF, band pass filter; EDFA, erbium doped fiber amplifier; ESA, electrical spectrum analyzer; HT, Hilbert transformer; LD, laser diode; PC, polarization controller; PPG, pulse pattern generator; PD, photodiode.

waveform generators (AWGs) using offline-processed waveform data. A 100 Mbit/s NRZ coded random sequence (PN length 10) was used as the baseband signal. The Hilbert-transformed signal was generated for different cut-off frequencies of $H_H(\omega)$. The baseband signal speed was restricted by the sampling frequency of AWG. The baseband signal and Hilbert-transformed signal were modulated onto the 1552.5 nm optical carrier by an LN vector modulator. An optical BPSK-VSB signal was generated by biasing two MZIs of the LN vector modulator to their transmission null points. The half-wave voltages of two sub-MZIs were 2.92 V. The baseband signal voltage was set as the modulation depth of 0.06. Small modulation depth was used by setting peak-to-peak driving signal voltages as smaller than 1 V to reduce the nonlinearity effect of the modulator. The modulator output signal was split into two parts using a 3 dB coupler. One of the two outputs of the 3 dB coupler was used to measure the optical waveform of the modulator output. The other was used to measure its power spectrum. The modulator output waveform was measured by connecting the upper photodiode (PD) output to a real-time oscilloscope. The light was amplified by an Erbium-doped fiber amplifier (EDFA) and was filtered for amplified spontaneous emission (ASE) noise before it was sent to the PD. Because of the difficulty in achieving high spectral resolution in optical domain, the spectrum of the modulator output signal was measured in electrical domain. Using self-heterodyne method, the spectrum was measured by an electrical spectrum analyzer. The other half of the modulator output signal was combined with a 120 MHz frequency shifted carrier at a 3 dB coupler. The frequency shift to the carrier was given by an acousto-optic switch of 120 MHz. After the combined light was amplified, the ASE noise was removed using an optical band pass filter. Then, the light was sent to a PD. The PD output was connected to the electrical spectrum analyzer to measure the spectrum.

3.2 Results and Discussion

Measured waveforms and power spectra are presented, respectively, in Figs. 9 and 10. Fig. 9(a) portrays waveforms obtained when $H_I(\omega)$ was used. Fig. 9(b)–(d) show the waveforms obtained when f_C values of the high-pass Hilbert transform were, respectively 10, 20, and 30 MHz. The modulator output waveform obtained when $H_I(\omega)$ was used (see Fig. 9(a)) consists of high peaks because of the peaky Hilbert- transformed waveform. In the high-pass Hilbert-transformed case, the peak-to-peak voltage of the Hilbert-transformed signal decreases along with cut-off frequency f_C. Peaks of the optical waveform at the modulator output started to decay accordingly, making the optical signal nonlinear tolerant. As predicted by the simulation results of Section 2, for the 100 Mbit/s baseband signal, the peak-to-peak voltage of the high-pass Hilbert-transformed signal became equal to that of the baseband signal at 30 MHz cut-off frequency. As discussed in Section 2, high-pass filtering of Hilbert-transformed signal removes the restriction on modulation depth. Therefore, a phase-shift method optical BPSK-VSB signal can be generated at higher modulation depths. This point also shows the capability of optical SNR adjustment of the modulator output signal

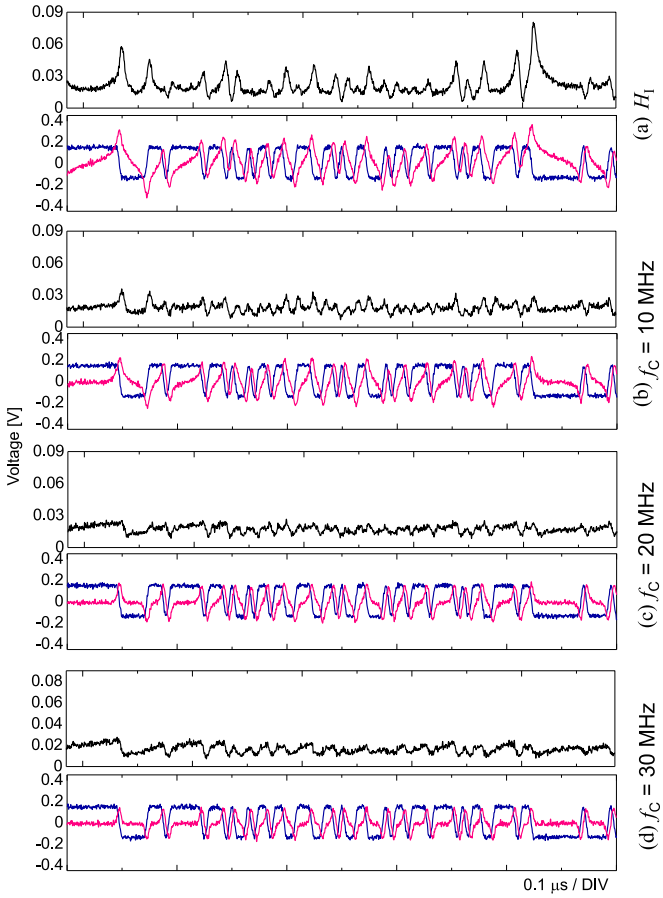

Fig. 9. Modulator input and output waveforms (bit rate: 100 Mbit/s): black, modulator output intensity waveform; blue, baseband signal waveform. pink, Hilbert-transformed signal waveform. (a) H_I. (b) to (d) are, respectively, H_H at $f_C =$ 10 MHz, $f_C =$ 20 MHz, and $f_C =$ 30 MHz.

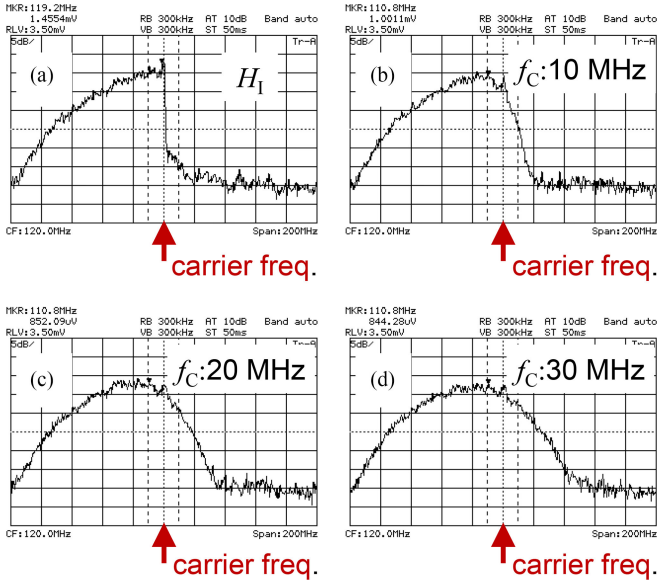

Fig. 10. Power spectra of modulator output signal (bit rate: 100 Mbit/s). (a) H_I. (b) to (d) are, respectively, H_H at $f_C =$ 10 MHz, $f_C =$ 20 MHz, and $f_C =$ 30 MHz.

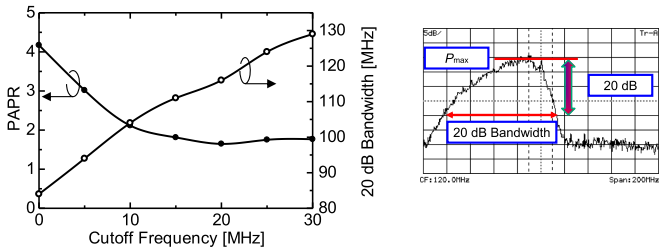

Fig. 11. PAPR and 20 dB bandwidth of phase-shift method optical BPSK-VSB signal. (Inset) Definition of 20 dB bandwidth.

according to the demands of the transmission system. The optical SNR of modulator output signal can be adjusted by choosing the appropriate cut-off frequency of the high-pass Hilbert transform.

Measured spectra of the modulator output signal are presented in Fig. 10. The power spectrum of optical BPSK-SSB signal presented in Fig. 10(a) shows ideal roll-off characteristics near the carrier frequency. The channel bandwidth was exactly the same as the baseband bandwidth. Fig. 10(b)–(d) present the spectra of phase-shift method optical BPSK-VSB signal at cut-off frequencies of 10, 20, and 30 MHz. Bandwidth of the modulator output signal spectrum widened with increasing cut-off frequency of $H_H(\omega)$. The SSB signal spectrum of Fig. 10(a) gradually transferred to the VSB signal spectrum when a high-pass Hilbert transform was applied.

Because PAPR of modulator output signal was a concern in optical BPSK-SSB modulation [29], [30], PAPR of the modulator output signal was measured and shown against the cut-off frequency of $H_H(\omega)$ in Fig. 11. The value of PAPR of the modulator output signal becomes 4.17 in the case where $H_I(\omega)$ was used. As a result of peak reduction in Hilbert-transformed waveform, PAPR of the modulator output signal decreases with cut-off frequency of $H_H(\omega)$. Actually, PAPR drops to 1.65 when the cut-off frequency of $H_H(\omega)$ at 20 MHz, giving reduction of 60.43% to PAPR of $H_I(\omega)$. At the cut-off frequency of 20 MHz, the measured $V_{\mathrm{pp-H}}$ became 1.11 times $V_{\mathrm{pp-B}}$. Because of the reduction of $V_{\mathrm{pp-H}}$, the modulation depth, which was restricted to 0.4 in optical BPSK-SSB modulation, can be increased to 0.9. At the cut-off frequency of 20 MHz, the modulation depth is 2.25 times greater than that of the optical BPSK-SSB signal.

When spectral efficiency is defined as the ratio of bit rate to channel bandwidth, spectral efficiency becomes 1 bit/s/Hz when $H_I(\omega)$ is used. With increasing cut-off frequency of $H_H(\omega)$, spectral efficiency decreases. Spectral efficiency of 0.71 bit/s/Hz is achieved at the cut-off frequency of 30 MHz. As shown in the inset of Fig. 11, 20 dB bandwidth is defined as the bandwidth of the modulator output signal spectrum, where the power spectrum density becomes -20 dB relative to the maximum power spectral density of the spectrum. The variation of 20 dB bandwidth with the cut-off frequency is also presented in Fig. 11. High-pass filtering of Hilbert-transformed signal reduces power of the lower frequency band of the Hilbert-transformed signal spectrum. This power reduction of the lower frequency band produces a vestigial sideband in the modulator output signal spectrum. Subsequently, 20 dB bandwidth increases almost linearly with the cut-off frequency of $H_H(\omega)$. It is noteworthy that more than 22% of bandwidth can be saved compared to double-sideband modulation, even at f_C of 30 MHz.

4. Fiber Transmission Characteristics

Because of the PAPR reduction of modulator output signal, the phase-shift method optical BPSK-VSB signal is expected to show tolerance to fiber nonlinearities relative to the optical BPSK-SSB signal. To study the fiber transmission characteristics of a phase-shift method optical BPSK-VSB signal, 100-km transmission simulation was conducted. Optical BPSK-VSB signal was generated using the transmitter model presented in Fig. 1(a). We assumed 10 Gbit/s single-channel transmission. Principally, there is no restriction on the transmission rate in the proposed scheme. However, increasing transmission rate requires faster DSP to implement the Hilbert transformer. The 10 Gbit/s

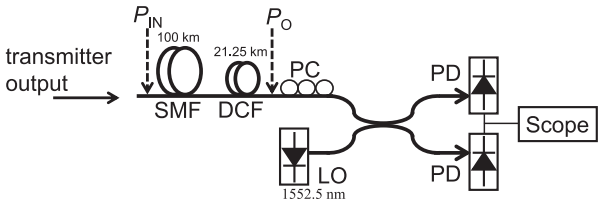

Fig. 12. Simulated fiber transmission setup: SMF, single mode fiber; DCF, dispersion compensating fiber; PC, polarization controller; PD, photodiode; LO, local oscillator.

TABLE 1
Fiber Parameters

Parameter		SMF	DCF	Unit
Loss coefficient	α	0.2	0.45	dB/km
Dispersion coefficient	D	+17.0	−80.0	ps/nm/km
Dispersion slope	S	0.057	−0.22	ps/nm^2/km
Effective core cross section	A_{eff}	80	14	μm^2
Nonlinear index coefficient	n_2	2.9×10^{-20}	4.3×10^{-20}	m^2/W

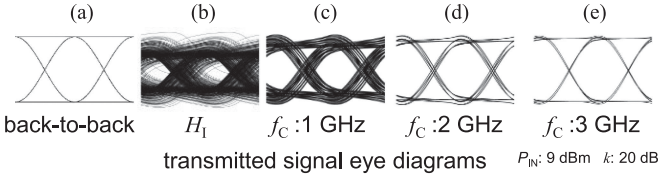

Fig. 13. (a) Back-to-back eye diagram of BPSK-VSB. (b)–(e) Transmitted signal eye diagrams: (b) H_I, (c) f_C: 1 GHz, (d) f_C: 2 GHz, and (e) f_C: 3 GHz.

NRZ coded baseband signal (PN length 10) was high-pass Hilbert transformed. The modulator was driven by the baseband signal and high-pass Hilbert transformed signal. The modulator output signal was launched into the fiber link (Fig. 12), which is 100 km of standard single mode fiber (SMF). In addition, 21.25-km of dispersion compensating fiber (DCF) was used to compensate the group velocity dispersion of SMF fiber after confirming a lack of waveform degradation during the dispersion compensating process. Because of the high sensitivity of coherent detection [31], optical amplifiers were not used in our transmission model. Here, P_{IN} and P_O respectively denote the average fiber input and output power. Fiber transmission was calculated by solving the nonlinear Schrödinger equation in split-step Fourier method [32] using the fiber parameters presented in Table 1. The transmitted signal was received by a phase-diversity homodyne detector. The receiver comprises a balanced detector and local oscillator (LO) laser. To clarify the effects of fiber nonlinearity on waveform degradations of optical BPSK-VSB signal, the LD and LO were assumed to have identical linewidths with perfectly matched phase. Fiber nonlinearity based waveform degradation is the dominant signal degradation factor in our transmission model. Therefore, instead of bit error rate (BER), we used eye diagrams of the received signal to evaluate the transmitted signal.

Optical BPSK-VSB signal eye diagrams of conditions before and after transmission at modulation depth of 0.1 are presented for comparison in Fig. 13. Fig. 13(a) is the back-to-back eye diagram; Fig. 13(b) shows the received signal eye diagram of phase-shift method optical BPSK-SSB

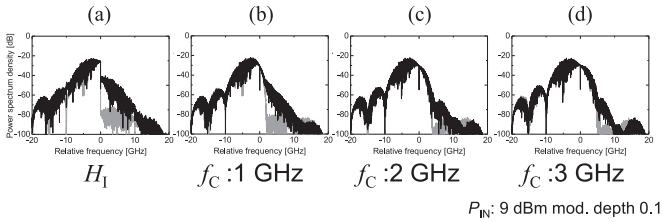

Fig. 14. Transmitted signal power spectra (black, after transmission. gray, before transmission). (a) H_I. (b)–(d) high-pass Hilbert-transformed (b) f_C: 1 GHz, (c) f_C: 2 GHz, and (d) f_C: 3 GHz.

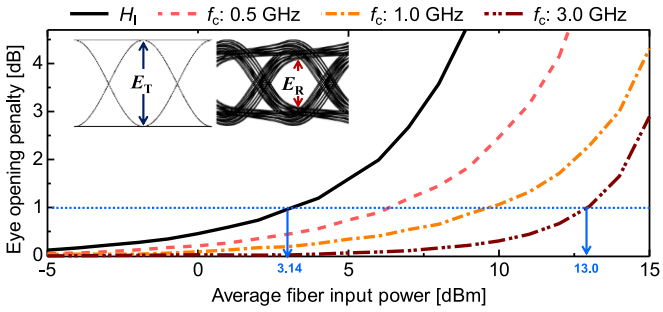

Fig. 15. Eye opening penalty of transmitted signal. (Inset) Definition of E_T and E_R.

transmission. We found no significant difference between back-to-back eye diagrams of different cut-off frequencies. Therefore, Fig. 13(a) represents all back-to-back eye diagrams. Fig. 13(c)–(e), respectively, present eye diagrams of the optical BPSK-VSB signal at cut-off frequencies of 1, 2, and 3 GHz. k is defined as the ratio of LO power to the received signal power. For calculations of transmitted signal eye diagrams, k was set to 20 dB and P_{IN} to 9 dBm. The high PAPR of optical BPSK-SSB degrades the received signal eye diagram because of nonlinear phase-shifts by SPM. In optical BPSK-VSB modulation, opened eye diagrams are noticed with increasing cut-off frequency. A similar eye diagram to the back-to-back eye diagram can be found for the cut-off frequency of 3 GHz.

Group velocity dispersion is fully compensated. The LO-LD phase is matched in the studied transmission link. Therefore, degradation appearing in eye diagrams can be inferred as attributable to fiber nonlinearities. PAPR of optical BPSK-VSB signal at cut-off frequency of 3 GHz becomes 1. Therefore, no marked degradation was found in the transmitted signal eye diagram. Power spectra of optical BPSK-VSB signal obtained before and after fiber transmission are presented for comparison in Fig. 14. Spectral degradation during the fiber transmission is notable in signals with high PAPR. Along with the cut-off frequency, spectral degradation of the optical BPSK-VSB signal lessens. No spectral degradation occurs in the main lobe of the transmitted signal spectrum at the cut-off frequency of 3 GHz.

To evaluate signal degradations of the transmitted signal, eye opening penalty (*EOP*) is defined as

$$EOP = \frac{E_R}{(\alpha_{SMF} L_{SMF} \times \alpha_{DCF} L_{DCF})\, E_T} \tag{3}$$

where E_R denotes the eye opening of transmitted signal, and E_T represents the eye opening of the back-to-back eye diagram when the modulation depth is 0.1. α and L are the loss coefficients and fiber lengths of SMF and DCF of transmission link. Fig. 15 shows the *EOP* of optical BPSK-VSB signal for different cut-off frequencies. E_R and E_T are presented in the inset. In optical BPSK-SSB signal, *EOP* increases dramatically with P_{IN}. Waveform degradation caused by SPM is the reason for this increase in *EOP*. In the optical BPSK-VSB signal, EOP for a given average fiber input power

becomes low when the cut-off frequency is increased. For evaluation, the value of the average fiber input power at which *EOP* becomes 1 dB is defined as the SPM threshold. Average fiber input power at SPM threshold is proportional to achievable transmission distance. Therefore, average fiber input power at SPM threshold can be used to compare the achievable transmission distance of different cut-off frequency scenarios. In the studied system, the SPM threshold of optical BPSK-SSB signal becomes 3.14 dBm for modulation depth of 0.1. In optical BPSK-VSB modulation, the SPM threshold can be improved to 13 dBm by setting the cut-off frequency of the high-pass Hilbert transformer to 3 GHz for a 10 Gbit/s NRZ coded signal.

5. Conclusions

We introduced a novel fiber nonlinearity tolerant modulation format using phase-shift method for medium/long-reach transmission. The proposed optical BPSK-VSB signal was generated using a modified Hilbert transformer, which can be implemented using DSP. The principle of the proposed method was tested experimentally and was evaluated. For the proof-of-principle experiment, an optical signal with minimum PAPR of 1.65 was generated by setting the cut-off frequency of high-pass Hilbert transformer at 20 MHz for 100 Mbit/s baseband signal. Other than the low PAPR of optical signal, the phase-shift method optical BPSK-VSB signal spectrum has less spurious spectral components. Channel bandwidth controllability of the proposed modulation scheme using DSP might be a special benefit in elastic optical network scenarios. Tolerance to fiber nonlinearity of the proposed optical BPSK-VSB signal was evaluated using numerical analysis in 100-km transmission link. It is noteworthy that fiber nonlinearity based signal distortions of optical BPSK-VSB signal can be minimized by adjustment of the cut-off frequency of the high-pass Hilbert transformer. By choosing the appropriate cut-off frequency of the high-pass Hilbert transformer, the SPM threshold of optical BPSK-VSB signal can be improved up to 13 dBm in the studied transmission link. The results of fiber transmission exhibit a tradeoff between the channel bandwidth and the tolerance to fiber nonlinearity in the proposed modulation scheme. However, suppression of the side lobe power (in the upper sideband of the spectrum) is expected to compensate for the reduced spectral efficiency by increased main lobe bandwidth in a WDM scenario.

Acknowledgment

The authors thank Y. Ichijo for computation help.

References

[1] A. D. Ellis, J. Zhao, and D. Cotter, "Approaching the non-linear Shannon limit," *J. Lightw. Technol.*, vol. 28, no. 4, pp. 423–433, Feb. 2010.
[2] G. Raybon and P. J. Winzer, "100 Gb/s Challenges and Solutions," presented at the Opt. Fiber Commun. Conf., San Diego, CA, USA, 2008, Paper OTuG1.
[3] W. Shieh, H. Bao, and Y. Tang, "Coherent optical OFDM: Theory and design," *Opt. Exp.*, vol. 16, no. 2, pp. 841–859, Jan. 2008.
[4] G. Bosco, V. Curri, A. Carena, P. Poggiolini, and F. Forghieri, "On the performance of Nyquist-WDM terabit superchannels based on PM-BPSK, PM-QPSK, PM-8QAM or PM-16QAM subcarriers," *J. Lightw. Technol.*, vol. 29, no. 1, pp. 53–61, Jan. 2011.
[5] X. Zhou and L. Nelson, "Advanced DSP for 400 Gb/s and beyond optical networks," *J. Lightw. Technol.*, vol. 32, no. 16, pp. 2716–2725, Aug. 2014.
[6] M. Mazurczyk, "Spectral shaping in long haul optical coherent systems with high spectral efficiency," *J. Lightw. Technol.*, vol. 32, no. 16, pp. 2915–2924, Aug. 2014.
[7] A. Dochhan, H. Griesser, N. Eiselt, M. H. Eiselt, and J.-P. Elbers, "Solutions for 80 km DWDM systems," *J. Lightw. Technol.*, vol. 34, no. 2, pp. 491–499, Jan. 2016.
[8] L. Sun, J. Du, and Z. He, "Multiband three-dimensional carrierless amplitude phase modulation for short reach optical communications," *J. Lightw. Technol.*, vol. 34, no. 13, pp. 3103–3109, Jul. 2016.
[9] J. L. Wei, J. D. Ingham, D. G. Cunningham, R. V. Penty, and I. H. White, "Performance and power dissipation comparisons between 28 Gb/s NRZ, PAM, CAP and Optical OFDM systems for data communication applications," *J. Lightw. Technol.*, vol. 30, no. 20, pp. 3273–3280, Oct. 2012.
[10] T. Tanaka *et al.*, "Experimental demonstration of 448-Gbps+ DMT transmission over 30-km SMF," presented at the Opt. Fiber Commun. Conf., San Francisco, CA, USA, 2014, Paper M2I.5.

[11] L. Zhang *et al.*, "Beyond 100-Gb/s transmission over 80-km SMF using direct-detection SSB-DMT at C-Band," *J. Lightw. Technol.*, vol. 34, no. 2, pp. 723–729, Jan. 2016.
[12] K. Yonenaga and N. Takachio, "A fiber chromatic dispersion compensation technique with an optical SSB transmission in optical homodyne detection systems," *IEEE Photon. Technol. Lett.*, vol. 5, no. 8, pp. 949–951, Aug. 1993.
[13] M. Sieben, J. Conradi, and D. E. Dodds, "Optical single sideband transmission at 10 Gb/s using only electrical dispersion compensation," *J. Lightw. Technol.*, vol. 17, no. 10, pp. 1742–1749, Oct. 1999.
[14] W. Idler, S. Bigo, Y. Frignac, B. Franz, and G. Veith, "Vestigial side band demultiplexing for ultra high capacity (0.64 bit/s/Hz) transmission of 128 $\times$ 40 Gb/s channels," presented at the Opt. Fiber Commun. Conf., Anaheim, CA, USA, 2001, Paper MM3–1.
[15] T. Tsuritani, A. Agata, I. Morita, K. Tanaka, and N. Edagawa, "Performance comparison between DSB and VSB signals in 20Gbit/s-based ultra-long-haul WDM systems," presented at the Opt. Fiber Commun. Conf., Anaheim, CA, USA, 2001, Paper MM5.
[16] S. Bigo, "Multiterabit/s DWDM terrestrial transmission with bandwidth-limiting optical filtering," *IEEE J. Sel. Topics Quantum Electron.*, vol. 10, no. 2, pp. 329–340, Mar. 2004.
[17] Y. Kim, S. Kim, I. Lee, and J. Jeong, "Optimization of transmission performance of 10-Gb/s optical vestigial sideband signals using electrical dispersion compensation by numerical simulation," *IEEE J. Sel. Topics Quantum Electron.*, vol. 10, no. 2, pp. 371–375, Mar. 2004.
[18] K. Schuh, E. Lach, B. Junginger, G. Veith, J. Renaudier, G. Charlet, and P. Tran, "8 Tbit/s (80 $\times$ 107 Gbit/s) DWDM ASK-NRZ VSB Transmission Over 510 km NZDSF With 1 bit/s/Hz Spectral Efficiency," presented at the Eur. Conf. Opt. Commun., Berlin, Germany, 2007, Paper PD1.8.
[19] R. -J. Essiambre, G. Kramer, P. J. Winzer, G. J. Foschini, and B. Goebel, "Capacity limits of optical fiber network," *J. Lightw. Technol.*, vol. 28, no. 4, pp. 662–701, Feb. 2010.
[20] T. Tsuritani, I. Morita, and N. Edagawa, "Study on PMD and dispersion tolerance of 20 Gbit/s VSB-RZ optical signal," presented at the 4th Pacific Rim Conf. Lasers and Electro-Optics, Chiba, Japan, 2001, Paper ThB1-3.
[21] M. Y. Frankel and R. D. Esman, "Optical single-sideband suppressed-carrier modulator for wide-band signal processing," *J. Lightw. Technol.*, vol. 16, no. 5, pp. 859–863, May 1998.
[22] P. J. Winzer and R.-J. Essiambre, "Advanced modulation formats for high-capacity optical transport networks," *J. Lightw. Technol.*, vol. 24, no. 12, pp. 4711–4728, Dec. 2006.
[23] K. Schuh, E. Lach, B. Junginger, and B. Franz, "53.5 Gbit/s NRZ-VSB modulation applying a single Mach–Zehnder modulator and transmission over 21 km SSMF with electronic dispersion compensation," presented at the Opt. Fiber Commun. Conf., San Diego, CA, USA, 2009, Paper OThC7.
[24] B. P. Lathi and Z. Ding, *Modern Digital and Analog Communication Systems*, New York, NY, USA: Oxford Univ. Press, 2009.
[25] P. Watts, R. Waegemans, M. Glick, P. Bayvel, and R. Killey, "An FPGA-based optical transmitter design using real-time DSP for advanced signal formats and electronic predistortion," *J. Lightw. Technol.*, vol. 25, no. 10, pp. 3089–3099, Oct. 2007.
[26] T. G. Nguyen *et al.*, "Integrated frequency comb source based Hilbert transformer for wideband microwave photonic phase analysis," *Opt. Exp.*, vol. 23, no. 17, pp. 22087–22097, Aug. 2015.
[27] K. I. A. Sampath, and K. Takano, "Optical VSB modulation based on phase-shift method and its PAPR characteristics for optical BPSK transmission," presented at the Optoelectron. and Commun. Conf. Opt. Fibre Technol., Melbourne, Australia, 2014, Paper WEPS2-55.
[28] K. Takano, Y. Naganuma, and K. Nakagawa, "Performance analysis of optical single sideband modulation based on Mach–Zehnder interferometers and its dispersive fiber transmission," *IEICE Trans. Commun.*, vol. E88-B, no. 5, pp. 1994–2003, May 2005.
[29] K. Takano, N. Sakamoto, and K. Nakagawa, "SPM effect on carrier-suppressed optical SSB transmission with NRZ and RZ formats," *Electron. Lett.*, vol. 40, no. 18, pp. 1150–1151, Sep. 2004.
[30] K. Takano, T. Murakami, Y. Sawaguchi, and K. Nakagawa, "Influence of self-phase modulation effect on waveform degradation and spectral broadening in optical BPSK-SSB fiber transmission," *Opt. Exp.*, vol. 19, no. 10, pp. 9699–9707, May 2011.
[31] B. Zhang, C. Malouin, and T. J. Schmidt, "Design of coherent receiver optical front end for unamplified applications," *Opt. Exp.*, vol. 20, no. 3, pp. 3225–3234, Jan. 2012.
[32] G. P. Agrawal, *Nonlinear Fiber Optics*, New York, NY, USA: Academic, 2010.